SRTTU

JCARME
Journal of Computational and Applied Research in Mechanical Engineering

http://jcarme.srttu.edu
ISSN: 2228-7922
Vol. 1, No. 2, March 2012

Application of the airflow control by electro-hydrodynamic actuator

R. Mestiri[a,*], F. Aloui[b] , R. Hadaji[c] and S. Ben Nasrallah[c]

[a]*LESTE, Ecole Nationale d'Ingénieurs de Monastir, Monastir, 5000, Tunisia.*
[b]*University of Valenciennes, ENSIAME, Lab. TEMPO (DF2T)- EA4542, Le Mont Houy, F- 59313 Valenciennes Cedex 9, France.*
[c] *Département de Génie Electrique, ENIM, Monastir, 5000, Tunisia.*

Article info:
Received: 22/10/2011
Accepted: 17/01/2012
Online: 03/03/2012

Keywords:
Airflow,
Boundary layer,
Corona discharge,
Electric wind,
Flow control,
Plasma actuator

Abstract
The technique used to control the airflow is based on the electro-hydrodynamic actuator which is also called plasma actuator. This actuator ensures the airflow control thanks to the electric wind created by the electrical corona discharge. This ionic wind is developed at the profile surface tangential to the initial free airflow so that it has a significant effect on the boundary layer flow. The studied profile was a NACA4412 airfoil. The electro-hydrodynamic actuator was placed at the surface of the NACA profile. The PIV visualizations made at angle of attack of 18° show an earlier flow reattachment to the profile surface when the plasma actuator is active. PIV measurements confirm that downstream of the actuator, when the discharge is ON, the wall velocity gradient is increased as illustrated by the velocity profiles taken at several positions on the NACA4412 wall. Then the plasma actuator can decrease the boundary layer thickness.

Nomenclature

c	chord length of the NACA4412 profile
I	corona current
Re_c	Reynolds number based on the NACA4412 chord length
U	x component of the airflow velocity
U_∞	free airflow velocity
V	Voltage
x	coordinate in the chord direction
Y	coordinate in the direction normal to the chord
z	coordinate in the spanwise direction
α	angle of attack of the NACA4412

*Corresponding author
Email address: rafika.mestiri@enim.rnu.tn

1. Introduction

The natural phenomena created at the taking off and the landing of plane can be suppressed or decreased by controlling the airflow around airfoils.
The used electro-hydrodynamic actuator is based on a direct current high voltage between the electrodes. The travelling positive ions between the electrodes transfer their momentum to the neutral particles of the fluid and at the same time act on the corona wire by a force against the drag direction due to the repelling

action between these positive ions and the positive electrode. The momentum gained by the fluid equals the acting force on the electrode and the drag will be reduced by a similar amount.

Airflow control around airfoils was studied by plasma actuators [1-5]. These studies showed that this kind of actuators can increase the lift and suppress the dynamic stall vortex.

Simplicity and fast-action of the plasma actuators make them efficient for aerodynamic applications [6-8]. An active drag-reduction technique was implemented by a dielectric barrier-discharge plasma actuator [9, 10]. Choi et al. [11] showed that plasma actuator can give up to 45 per cent skin-friction reduction.

The biconvex and non symmetric NACA4412 profile has been the subject of several numerical and experimental studies.

Indeed, numerical studies of the flow over a NACA4412 airfoil were done at maximum lift with incidence angle of 13.87° for a Reynolds number, of Re_c=1.52 x 10^6 [12-13]. These results compared well with the experimental data of Coles et al. [14] and with the well established numerical results of Thomas *et al.* [15]. The early experimental studies [14, 16, and 17] on the flow around NACA4412 airfoil demonstrated that the maximum lift happens at the angle of 13.87°, but the later studies confirmed that the angle was 12°. Wadcock [17] reported that the early data showed by Coles *et al.* [14] agree very well with his new data at 12°, suggesting that the early experiment [14] suffered from a non-parallel mean flow in the Caltech wind tunnel. It should be pointed out that the Reynolds-averaged simulations are usually run at 13.87° and do not agree with the data when run at 12° [17]. The flow configuration chosen by Jansen [18] was that of Wadcock [17] at Reynolds number of Rec=1.64x 10^6, Mach number of M=0.2 and ange of attack of 120. From the stagnation point on the leading edge of the NACA4412 airfoil, thin laminar boundary layers form in a very favourable pressure gradient. This pressure gradient then turns adverse, leading to flow separation. Only the onset of turbulence can cause the flow to remain attached or to reattach. The persistent adverse pressure gradient eventually leads to turbulent flow separation in the last 20 percent of the airfoil chord [18].

When the angle of attack increases, the friction drag has only a minor change. On the other hand, the pressure drag increases quickly when the boundary layer separation occurs on the suction surface of the profile, accompanied with the formation of a separation bubble at constant pressure. In these unstable zones, modelling is difficult and hardly reliable [19].

Controlling the aerodynamics of the flow over an airfoil is sought to enhance the capabilities of the next-generation airplanes, which is a great challenge. The airflow over a NACA4412 profile is of special interest because it turns very fast from laminar to turbulent. Experimental studies using oscillatory jets for the active airflow control over a NACA4412 airfoil showed that the zero net-mass flow actuator placed at the leading edge of the airfoil was able to suppress leading edge separation for incipient and fully separated cases. The actuator can keep the flow attached although it is turbulent and incipiently separated. The flow remains attached for at least 3 degrees over the incipient condition (α = 15°) with a moderate input voltage in the speakers [20-22].

In this paper, we will present the experimental results of the airflow control around a NACA4412 airfoil using an electro-hydrodynamic actuator. PIV (Particle Image Velocity) measurements are performed on the airflow around the NACA4412 profile with and without actuation.

2. Experimental setup

The experiments were conducted in a subsonic wind tunnel (Fig. 1). The open wind tunnel has a test section of 0.68 m (width)×0.68 m (height)×0.38 m (length). The NACA4412 was placed in the tunnel as shown in Fig. 1. In the measurement section, the tunnel walls are made of transparent Plexiglass for flow visualization and PIV measurement. The wind velocity in the test section can be set up to 8.5 m/s. Three dimensional effects from tip vortices and the channel walls are reduced to a negligible level by locating the measurement window far from the airfoil ends and test section walls (at the

middle of airfoil span). All measurements were done with and without electrical discharge.

2.1. Airfoil

The airfoil used in this study was a NACA4412. This dissymmetric test model was designed to meet several requirements [23]. It is made of an assembly of two materials. The central part, having a width of 100 mm, is made of transparent Plexiglass (for PIV visualization) and the two adjacent parts are made of an insulating material. The airfoil has the following dimensions: a chord of 200 mm, a span of 670 mm and a maximum thickness of 23 mm (Fig. 2).

2.2. Plasma actuator

We used a High Voltage Generator (HVG) that provides a direct voltage up to 60 kV with a current of 2 mA (maximum power of 120 W). The DC (Direct Current) electrical discharge is generated when we apply a DC High Voltage at the anode keeping the cathode connected to the ground (Fig. 3). We placed two multi-meters to control the current and the voltage values. The plasma actuator consisted of two parallel copper electrodes spaced with 40 mm. The length of the used electrodes was 400 mm. The diameter of the anode was 0.6 mm and for the cathode it was 2 mm. This configuration for the plasma actuator was chosen after several tests. It was found to be the optimum configuration that provides a stable discharge with maximum corona current and electric wind. During the tests of the corona discharge stability, we had visualized the electric wind by a candle placed downstream the actuator and near the trailing edge. We placed our plasma actuator at the suction face of the NACA profile in order to control the boundary layer flow. The two electrodes were glued centrally over the airfoil span and the profile was fixed at a height of 0.3 m from the wind tunnel bottom. The actuator position is expressed in percent of x/c, where x is the distance from the leading edge and c is the chord length.

2.3. Measurements and visualizations

A standard Particle Image Velocimetry system was used to measure the velocity field around the foil. Measurements are taken in the symmetry plane of the airfoil (Fig. 2.a), i.e. in a region where the flow is assumed to be two-dimensional. For flow visualization, LAVISION smoke generator was used.

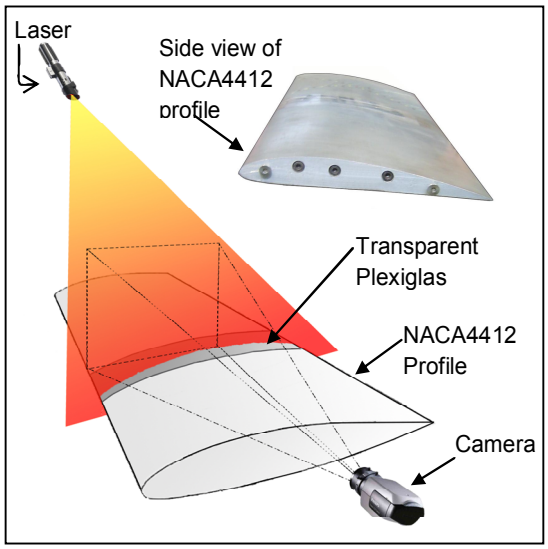

Fig. 1. The experimental set-up: Diagram of the PIV system.

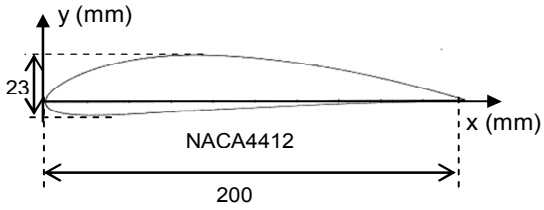

Fig. 2. Cross section of the NACA4412 profile.

Smoke was injected upstream of the airfoil. The airfoil was illuminated by a 15 Hz pulsed laser light source of type ND-Yag (532 nm, 160 mJ). This laser repetition frequency is suitable for the used free airstream velocity. Images were taken by a LAVISION Imager ProX classic camera (1600×1200 pixels). The PIV set up is shown in figure 1.
Visualizations were also made by introducing continuous smoke streak lines produced by incense tubes located at the spanwise centreline. The smoke streaks were vertically aligned along the mean flow direction. PIV treatments associated to the done measurements are made with interrogation windows of 32x32 pixels and an overlap of 50%.

3. Results and discussions

The NACA4412 was positioned with angles of attack between 15° and 18°. All the measurements were done inside the wind channel. So, it was necessary to make special surrounding conditions, such as keeping dielectric interior wall, in order to obtain a stable discharge without sparks. Also, when we use smoke, we must clean electrodes regularly, because the oil deposits on the electrodes, and it makes an unstable discharge. The oil deposits may cause the formation of electric arcs characterized by an abrupt increase of the corona current and a weak electric wind. When we lighted the discharge, we proceeded by a progressive increase of the high voltage until appearance of little sparks. So, we remade another time while stopping the voltage value corresponding to maximum current without any spark. Finally we made the PIV acquisition.

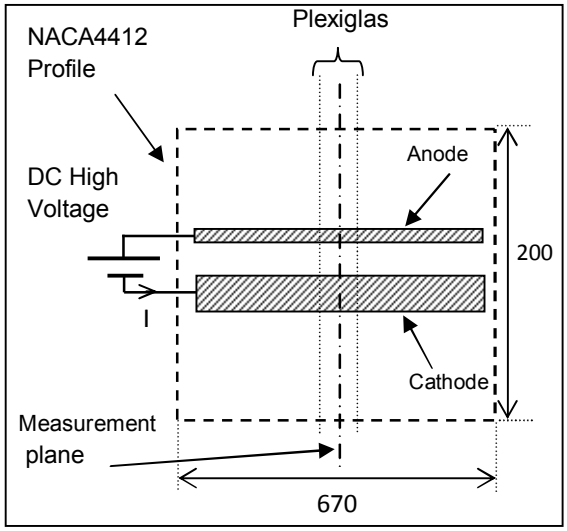

Fig. 3. Sketch of the top view of plasma actuator used in our experiments (dimensions in mm).

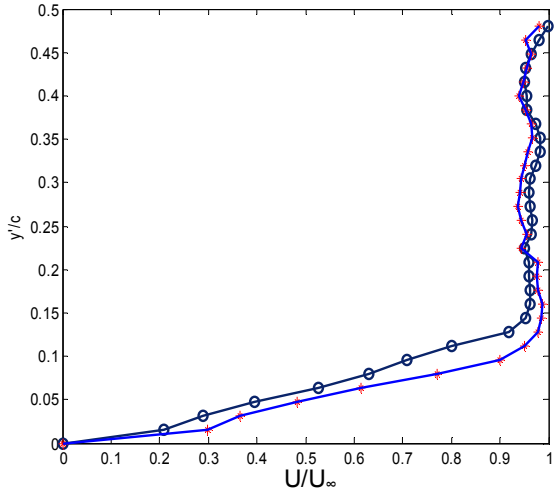

Fig. 4. Dimensional velocity profiles with (—*—) and without (—o—) corona discharge at x/c= 30%.

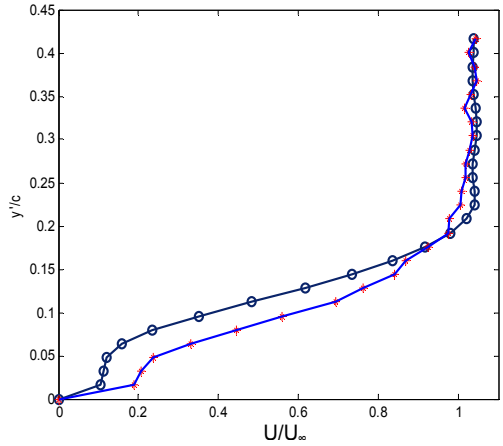

Fig. 5. Dimensionless velocity profiles with (—*—) and without (—o—) corona discharge at x/c= 50%.

3.1. Velocity profiles

In this paragraph, the velocity profiles are presented within the boundary layer of the NACA4412 profile at an angle of attack equal to 15° and for free airstream velocity of 1 m/s (Figs. 4-7). The Reynolds number based on the chord length was $Re_c = u_\infty c/\nu = 1.28 \times 10^4$. Plasma actuator was placed at x/c= 20% from the leading edge. The obtained non-dimensionalised velocity profiles, present the y/c as a function of U/U_∞, where y is the axis normal to the airfoil surface. Velocity profiles are given at four positions along the chord length: between the two electrodes (x/c= 30%), at the medium of the chord (x/c= 50%), a point at x/c= 65% and a last point close to the trailing edge at x/c= 85%.

This study allows us to see the evolution of the corona discharge effect intensity as a function of the distance from the electrodes. These profiles were taken when the plasma actuator was OFF and ON in order to show its effect on the free airstream above the NACA profile. The electrodes were set in such away to create an electric wind along the direction of the fluid flow (co-flow mode). The electric potential was 31 kV and the corona current was 40 µA.

The corona discharge modifies the velocity profile at the vicinity of the wall as we can observe in Figs. 4-7. The corona upstream the cathode, we remark a velocity increase about 0.1U00. At x/c= 50% and x/c= 65%, the added velocity is about 0.2U00. Near the trailing edge, which is the furthest point from the actuator, the discharge can accelerate the airflow at the vicinity of the profile surface by about 0.1U00.

The added velocity is due to the electric wind created tangentially to the NACA profile surface. According to the cases indicated in this paragraph, we note that the maximum of the electric wind velocity is downstream the electro-hydrodynamic actuator, at x/c=50% and x/c=65%. At x/c= 85%, the corona effect is less accentuated. We also note that for the velocity profiles without corona discharge effect, there is a point at which the velocity temporarily remains constant. This point appears at about y= 3 mm. This behaviour is more noticeable near the trailing edge. When the discharge is ON, this behavior does not exist anymore and the velocity profiles become more typical. Hence discharge improves the flow quality above the airfoil.

3.2. Effect on boundary layer thickness

Figure 8 shows the longitudinal evolution of the boundary layer thickness with and without corona effect. Corona discharge creates an electric wind which adds momentum to the fluid flow inside the boundary layer. This added momentum decreases the viscous effects in such away that reduces the total drag on the fluid. The plotted boundary layers are inferred from the velocity profiles presented in the preceding paragraph. The boundary layer thickness is the height measured from the wall to the point where the velocity equals 99% of the free stream velocity [24]. When the plasma actuator is ON, the boundary layer is thinned due to the added momentum, which increases the fluid velocity inside the boundary layer. This increase in velocity is accompanied by a reduction in the boundary layer thickness to keep the same mass flow throughout the boundary layer.

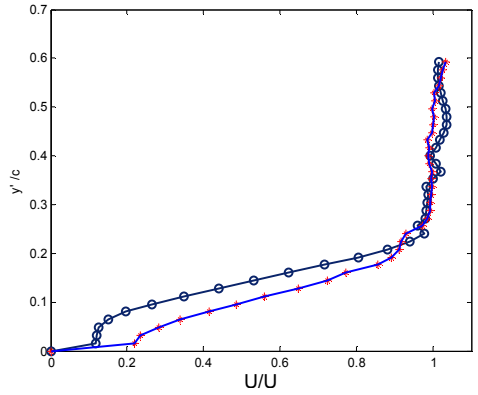

Fig. 6. Dimensionless velocity profiles with (—*—) and without (—o—) corona discharge at x/c= 65%.

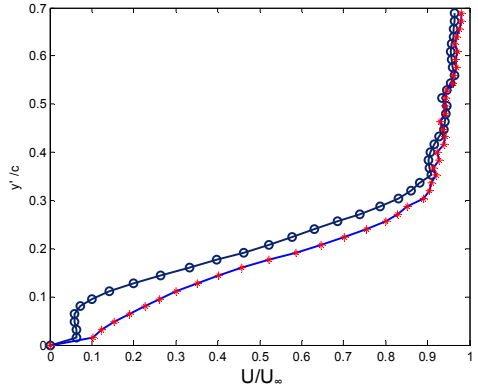

Fig. 7. Dimensionless velocity profiles with (—*—) and without (—o—) corona discharge at x/c= 85%.

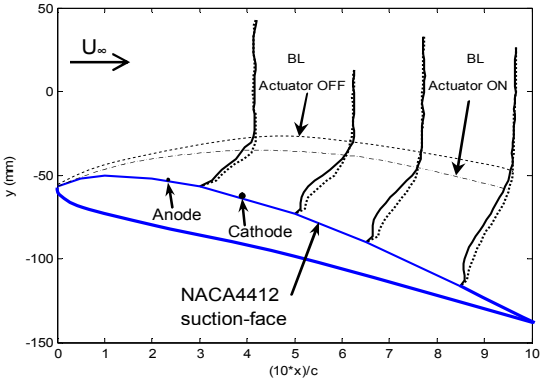

Fig. 8. Boundary Layer (BL) thickness without and with corona effect and the velocity profiles along the NACA4412 chord (U_∞= 1 m/s, c= 20 cm, anode is upstream).

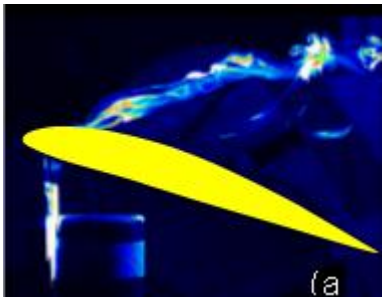

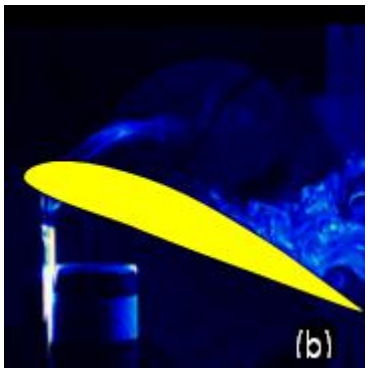

Fig. 9. Flow visualizations; V = 32 kV, I = 48 μA and plasma actuator placed at x/c=20%.

3.3. Visualizations

We investigated the effect of the electric wind by visualizing its consequence on incense smoke streaks. Visualizations were made with and without free airflow. In the case of actuation with a free airflow, results are shown in Fig. 9 for an airstream velocity of 0.6 m/s and the angle of attack of α= 18°. We observe that the flow is aspirated by the effect of the electric wind producing flow reattachment to the profile surface.

4. Conclusions

In this paper, we have presented a qualitative and quantitative PIV study of the airflow control above a NACA4412 profile. The qualitative results showed the response of the separated boundary layer to the forcing of the

DC corona discharge flow control. The data exhibit an important modification of the flow at the surface of a NACA4412 by the action of the electrical corona discharge.
The visualization by incense showed that the discharge aspirated the smoke to the NACA profile surface. We concluded that the electro-hydrodynamic actuator had the capability of keeping the flow attached to the airfoil surface.
Velocity profiles made with and without discharge effect showed that the plasma actuator increase the tangential velocity. This effect is decreased towards the trailing edge. Increase of velocity on the surface can delay the flow separation on the airfoil, which is the required flow control.

References

[1] L. Post and T. C. Corke "Separation control using plasma actuators: Dynamic stall vortex control on oscillating airfoil", *AIAA Journal*, Vol. 44, (2006).

[2] T. C. Corke, C. He and M. P. Patel "Plasma Flaps and Slats: an application of weakly-ionized Plasma actuators," *AIAA Paper 2004-2127,* (2004).

[3] D. K.Van Ness II, T. C. Corke and S. C. Morris "Turbine Tip Clearance Flow Control using plasma Actuators", *AIAA Paper 2006-21*, (2006).

[4] M. Forte, J. Jolibois, E. Moreau and G. Touchard "Optimization of a Dielectric Barrier Discharge actuator stationary and non-stationary measurements of the induced flow velocity- Application to airflow control," *3rd AIAA Flow Control Conference, AIAA Paper 2006-2863,* San Francisco, California, (2006).

[5] J. Jolibois, N. Bénard and E. Moreau "Contrôle de la traînée et de la portance d'un profil NACA0015 par actionneur plasma à décharge à barrière diélectrique", *43rd colloque d'Aérodynamique Appliquée*, Poitiers, (2008).

[6] E. Moreau "Airflow control by non-thermal plasma actuators", *J. Phys. D Appl. Phys.* Vol. 40, pp. 605-636, (2007).

[7] T. C. Corke, C. L. Enloe and S. P. Wilkinson "Dielectric barrier discharge plasma actuators for flow control", *Annu. Rev. Fluid Mech*, Vol. 42, pp. 505-530, (2010).

[8] T. C. Corke, P. O. Bowles, C. He and E. H. Matlis "Sensing and control of flow separation using plasma actuators", *Phil. Trans. R. Soc. A*, Vol. 369, pp. 1459-1475, (2011).

[9] R. Whalley and K. S. Choi "Starting, traveling and colliding vortices: dielectric-barrier discharge plasma in quiescent air", *Phys. Fluids*, Vol. 22, 091105, (2010).

[10] R. Whalley and K. S. Choi "Turbulent boundary layer control by DBD plasma: a spanwise travelling wave", *Proc. 5th AIAA Flow Control Conference,* Chicago, IL, 28 June–1 July 2010. AIAA Paper 2010-4840, (2010).

[11] K. S. Choi, T. Jukes and R. Whalley, "Turbulent boundary-layer control with plasma actuators", *Phil. Trans. R. Soc. A*, Vol. 369, pp. 1443-1458, (2011).

[12] A. Corsini, F. Rispoli and A. santoriello "A variational multiscale higher-order finite element formulation for turbomachinery flow computations", *Journal of Computer methods in applied mechanics and engineering*, Vol. 194, pp. 4797-4823, (2005).

[13] W. K. Anderson, R. D. Rausch and D. L. Bonhaus "Implicit/ Multigrid algorithms for incompressible turbulent flows on unstructured grids", *Journal of Computational Physics*, Vol. 128, pp. 391-408, (1996).

[14] D. Coles and A. J. wadcock "Flying hot-wire study of flow past an NACA 4412 airflow maximum lift", *AIAA Journal*, Vol. 17, pp. 321-329, (1979).

[15] J. Thomas, S. Krist and W. Anderson "Navier-Stokes Computations of Vortical Flows Over Low-Aspect-Ratio Wings", *AIAA Journal*, Vol. 28, pp. 205-212, (1990).

[16] R. C. Hastings and B. R. Williams "Studies of the flow field near a NACA 4412 aerofoil at nearly maximum lift",

Aeronautical Journal, Vol. 91, pp. 29-44, (1987).

[17] A. J. Wadcock "Investigation of low-speed turbulent separated flow around Airfoils", *NACA CR 177450*, (1987).

[18] K. Jansen "Preliminary large-eddy simulations of flow around a NACA 4412 airfoil using unstructured grids," Center for turbulent research, *Annual Research Briefs*, pp. 61-72, (1995).

[19] R. Rey and R. Noguera "Pofils, grilles d'aubes et machines axiales- tome II ", *Aero-hydrodynamique interne des machines, uee pa6* – ifmat et master imce, arts et metiers Paris Tech, pp. 41-42, (2008).

[20] M. Y. Andino, J. M. Ausseur, J. T. Pinier, M. N. Glauser and H. Higuchi "Interactions of Zero Net-Mass Flow Actuators the Flow over NACA 4412 Foils", *44th AIAA Aerospace Sciences Meeting and Exhibits, Nevada*, AIAA paper 2006-105, (2006).

[21] M. N. Glauser, H. Higuchi, J. Ausseur, J. Pinier and H. Carlson "Feedback Control of Separated Flows (Invited)", *2nd AIAA Flow Control Conference*, *Portland, Oregon,* AIAA Paper 2004-2521, (2004).

[22] J. M. Ausseur, J. T. Pinier, "Towards Closed-Loop feedback Control of the Flow over NACA-4412 Airfoil", *43ème AIAA Aerospace Sciences Meeting and Exhibit*, *Reno, Nevada*, AIAA Paper 2005-343, (2005).

[23] M. N. Glauser, M. J. Young, H. Higuchi and C. E. Tinney "POD Based Experimental Flow Control on a NACA-4412 Airfoil (Invited)", *42nd AIAA Aerospace Sciences Meeting and Exhibit, Reno,* AIAA Paper 2004-0575, (2004).

[24] S. H. El- Khabiry "*Numerical evaluation of corona discharge as a means of boundary layer control and drag reduction*," Ph.D. thesis, Iowa State University, Ames, Iowa, (1994).